Development of Porous Emitter Electrospray Thruster Using Advanced Manufacturing Processes

IEPC-2022-603

Presented at the 37th International Electric Propulsion Conference
MIT • Boston, USA
June 19-23, 2022

Arsad Quraishi[1], Szymon Dworski[2], Chengyu Ma[3],and Charles N. Ryan[4]
David Fearn Electric Propulsion Laboratory, Department of Aeronautics and Astronautics, University of Southampton, Southampton, United Kingdom

Alessandro Ferreri[5], Guillaume Vincent[6], Hugo Larsen[7], Emmanuelle Rosati Azevedo[8], Emily Dingle[9], and Alberto Garbayo[10]
AVS UK, Harwell Space Cluster, Oxfordshire, United Kingdom

Maria Vozarova[11] and Erich Neubauer[12]
RHP Technology, Austria

A UK-Austrian consortium led by AVS UK in collaboration with the University of Southampton (UoS) and RHP Technology is developing a low power porous electrospray propulsion system. Using as a baseline a thruster previously developed at UoS, the updated system design focuses on achieving higher thrust using processes suitable for high volume production. This is to meet the rapidly growing micro/nanosatellite market demand. Relying on more than 10 years of expertise in electrospray propulsion, UoS is leading the experimental test campaign and is assisting with thruster design. RHP Technology are creating the high-precision, high-volume manufacturing processes for the emitter arrays and the porous reservoir. AVS UK is designing the propulsion unit and associated High Voltage Power Processing Unit (HV-PPU) while also leading commercial exploitation. The two-year project is centred on three main goals. The first is to develop a thruster with improved performance metrics that better suit the new requirements of the micro/nanosatellite market. The second is to design an updated HV-PPU adapted to operate alongside the improved thruster. The third is to move away from the use of CNC machining in favour of sintering techniques for the manufacturing of the emitters. This paper describes the steps taken to achieve these goals with a particular emphasis on the emitter manufacturing and testing. Our initial single emitter tests demonstrate promising performance. A new single emitter demonstrated reasonably high emission current after onset, with maximum values of around 35 µA at ± 3500 V reached. Assuming a 50 % monomer-dimer mix, the estimated thrust and specific impulse are approximately ~3.50 µN and ~4600 s.

[1] Research Fellow, Department of Aeronautics and Astronautics, a.quraishi@soton.ac.uk
[2] Ph.D. Student, Department of Aeronautics and Astronautics, s.dworski@soton.ac.uk
[3] Research Fellow, Department of Aeronautics and Astronautics, chengyu.ma@soton.ac.uk
[4] Lecturer, Department of Aeronautics and Astronautics, c.n.ryan@soton.ac.uk
[5] Propulsion System Engineer, AV UK, aferreri@a-v-s.uk
[6] Electronics Engineer, AVS UK, gvincent@a-v-s.uk
[7] Mechanical Engineer, AVS UK, hlarsen@a-v-s.uk
[8] Propulsion Engineer, AVS UK, erosati@a-v-s.uk
[9] Head of Operations and Programmes, AVS UK, edingle@a-v-s.uk
[10] CEO, AVS UK, agarbayo@a-v-s.uk
[11] Material Researcher, RHP Austria, maria.vozarova@stuba.sk
[12] Managing Director, RHP Austria, e.ne@rhp.at

1. Introduction

In the past decade, nanosatellites (e.g., satellites with a mass of 1–20 kg) have become increasingly popular and now account for a significant portion of global satellite launches [1]. Developing capable and specifically tailored propulsion solutions for nanosatellites is important to further maximize the abilities of these platforms, enabling functionalities that include (1) maintaining relative positioning of satellites in a constellation (station keeping), (2) placement of satellites in a proper orbit (orbit establishment), (3) drag compensation, and (4) end of life maneuvering (either deorbit or transfer to a safe orbit). Several experimental propulsion systems have already been deployed on such nanosatellites, see for example [2, 3, 4]. A number of very low power electric propulsion (EP) systems are also currently being developed. These include plasma thrusters [5] and vacuum arc thrusters [6, 7, 8]. Space proven EP systems such as Hall Effect thrusters (HET) [9] and gridded ion thrusters [10, 11] have been successfully used on larger spacecraft with a power budget of 0.3–5 kW [9]. However, such systems cannot be easily scaled down to operate at the power level of a few dozen watts available for nanosatellite propulsion [12] as the efficiency of these devices drops dramatically with power [13]. In recent years, there has been an upsurge in research work around the world to develop new low power EP systems suitable for nanosatellites.

Another class of thruster that can be considered for nanosatellite applications is electrospray thrusters [14, 15, 16, 17, 18, 19]. These use a strong electric field to extract and accelerate particles from the surface of a liquid propellant. The design of an electrospray thruster is relatively simple, consisting of a propellant storage unit, a propellant transport system, an electrospray emitter and generally one electrode grid referred to as the extractor. One such thruster termed the "Porous-emitter Electrospray Thruster" (PET) has been developed and tested at the University of Southampton's David Fearn Electric Propulsion Lab [20, 21, 22, 23]. Further development of the PET thruster is now occurring in collaboration with RHP Technology (Austria) and AVS UK. The collaboration, funded through a ~£1.7M grant sponsored by the EUREKA SMART Programme for Advanced Manufacturing, brings together expertise in nanosatellite propulsion from academia and industry. RHP Technology bring unique skills and expertise in advanced manufacturing, especially concerning ceramic sintering of complex components. Within the project their role is to develop the porous emitters and reservoirs using additive manufacturing and powder injection moulding sintering techniques. AVS UK is responsible for the design of a flight-ready PET thruster, is developing the associated Power Processing Unit (PPU) and is leading the end commercial exploitation of the technology. The University of Southampton (UoS) is leading the testing as well as contributing to the design of the thruster.

2. Thruster Overview

The PET prototype previously developed at UoS consists of an extractor electrode, a porous emitter with 100 tips, a porous propellant reservoir, and a perforated aluminium electrode. All the thruster components are stacked inside a casing, which is additively manufactured via 3D printing using a high-detail resin material, while the extractor is mounted outside the thruster enclosure. The UoS thruster prototype in its current configuration (see Table 1) generates a thrust and I_{sp} of 263.5 μN and 3891 s respectively with 13 W input power [22]. Compared to other electric micro-propulsion systems [24, 25] for nanosatellites, the PET prototype has competitive propulsive performance. A propulsion system comprised of multiple thruster units could provide further enhanced performance. The goal of the present research is to develop a nanosatellite propulsion system producing thrust in the order of ~ 1 mN, with a total impulse of 5000 Ns (as recommended for LEO (Low Earth Orbit) small satellite constellations), and a maximum power consumption of 50 W. A summary of targeted performance for the updated PET system (hereafter referred as PET-50) is reported in Table 1.

Table 1. Summary of Targeted Performance.

Performance Parameter	PET Prototype at UoS [22]	Target Value, PET-50
Specific Impulse	3891 s	1700 s – 2400 s
Thrust	263.5 μN	~1 mN
Total Impulse	-	2000 Ns – 5000 Ns
Power	~13 W	~50 W
Wet Mass	-	~1.5 kg
Volume	4 x 4 x 2 cm^3	1 U (10 x 10 x 10 cm^3)

Four prototype PET thruster units operating together would be able to achieve 1.054 mN with a power consumption of 52 W whilst fitting within 1U. The PPU under development is expected to have an efficiency of ~70 % and accordingly we would expect total power requirements for the prototype thruster-PPU assembly to be ~ 74 W, i.e. more than the

targeted value. Hence, further work is ongoing to optimize the performance of the thruster and to lower the power demand. One aspect of improving the performance is to update the emitter geometry and the number of emitters per PET unit. CNC manufacturing was previously used to machine the emitter array from a 7.5 ± 0.2-mm thick borosilicate porous glass disc with a diameter of 120 mm sourced from VWR International LLC. This fabrication method results in a non-uniform emission affecting the overall beam current and subsequently the thrust yield. Therefore, emitter fabrication is being changed from CNC manufacturing to sintering. The performance of the sintered single emitters is currently being evaluated. Bearing in mind the targeted performance and power consumption values included in Table 1, the total number of emitters will be determined once this performance data has been fully collected. The updated PET-50 thruster is expected to have a higher thrust to power ratio and to be suitable for mass production thus fulfilling the rapidly growing nanosatellite market demand. An overview of the PET-50 is presented in Figure 1.

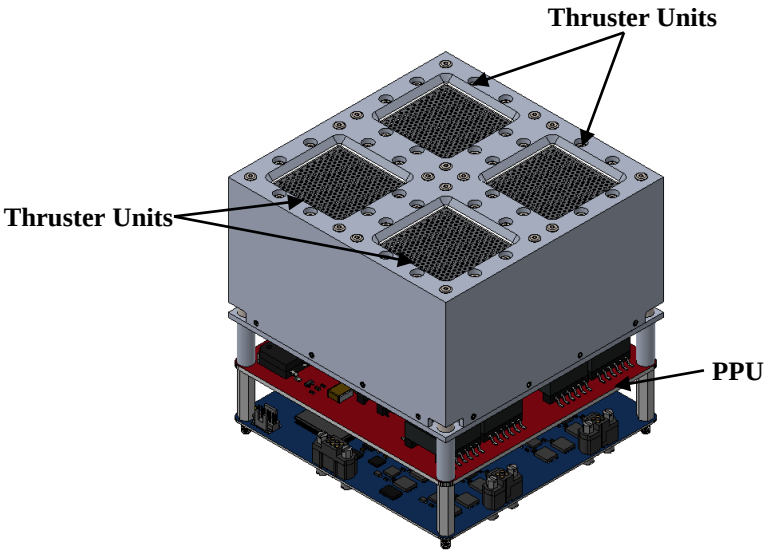

Figure 1: PET-50 thruster design overview.

The modified PET-50 thruster incorporates four thruster units. These units consist of a sintered emitter array, an extractor grid, and a propellant reservoir grouped together within an external aluminium housing. The PPU, consisting of a low voltage (blue) and high voltage (red) board is positioned upstream (at the bottom of Figure 1). It powers all the thruster units. The whole system is designed to occupy 1U.

3. Thruster Emitters Manufacturing

The design of electrospray emitters plays a crucial role in estimating thruster performance in terms of operational voltage, emission current, thrust, propellant transport method, and thruster lifetime. The development of emitters with reliable and stable performance requires the use of porous materials capable of transporting the liquid propellant via capillary forces. The following section describes the manufacturing of the emitters.

UoS are investigating the use of various emitter manufacturing techniques to produce the non-conductive emitter arrays in close collaboration with sintered component manufacturing experts RHP Technology. Techniques such as stereolithography (SLA), ceramic injection moulding (CIM), and cold-pressed bodies manufacturing (CPBM) are being investigated. The use of five powders of different qualities has been explored. The quality of the powder influences the porosity as well as the resolution of the final parts. This means careful consideration of the choice of powder is necessary. The methodology (and powder) which combines the best dimensional accuracy with corresponding porosity will be selected based on experimental thruster testing results. In the case of SLA, CIM, and CPBM all emitters containing organic binder are debound and sintered at temperatures up to 1500 °C.

3.1. Stereolithography - SLA

Stereolithography (SLA) is an additive manufacturing method [26] used for the production of parts with complex designs. It reduces manufacturing costs and produces parts with premium quality. The shaping process is based on the principle

of photopolymerization. The 3D objects are created using a light-emitting device (laser or digital light processing) that illuminates and cures a liquid photopolymer resin containing ceramic filler. A light source consisting of a LED lamp in conjunction with a liquid crystal display panel or a deformable mirror device (DMD) exposes an entire layer of photopolymer at one time. After the photopolymer is exposed to UV light from below through a transparent window, the fabricated part is pulled out of the vat and a new layer of the ink is deposited, as depicted in the Figure 2. SLA has the ability to produce fine features and provide a very good surface finish with minimum stair stepping effect [27, 28].

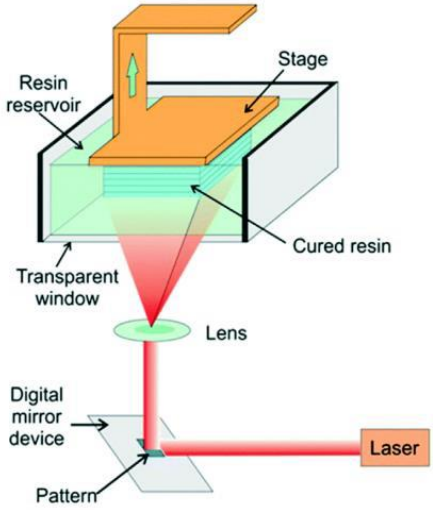

Figure 2: The typical implementation of SLA for rapid prototyping of ceramics-bottom up systems with digital light projection [29].

Three photosensitive inks containing high purity alumina powders with particle sizes from several nm up to 30 µm were used for emitter manufacturing. These suspensions were specially made for the additive manufacturing of the high-performance ceramics with SLA technology. The first prototype of the PET emitter array manufactured is shown in Figure 3.

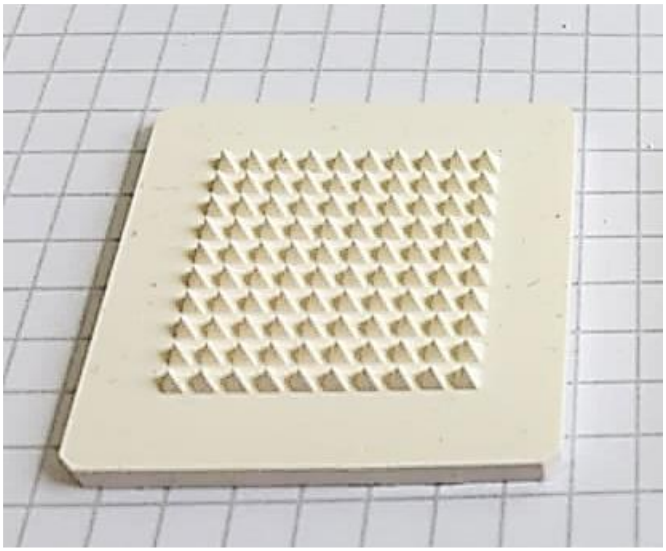

Figure 3: Image of a PET emitter array prepared by SLA.

3.2. Ceramic Injection Moulding- CIM

Ceramic injection moulding (CIM) is one of the techniques being investigated by the consortium for fabricating emitters with precise shapes from ceramic powder. The potential of CIM lies in its ability to combine the design flexibility of

plastic injection moulding with the nearly unlimited choice of material offered by the market, making it possible to combine multiple parts into a single one without excessive waste of material.

The starting material for CIM, usually termed feedstock, is a homogeneous granulated mixture of ceramic powder and an organic multi-component thermoplastic binder. The binder and the powder are combined and homogenized in mixing and extruding devices. The mixture is then granulated into appropriately sized granules that are fed into the injection moulding machine and injected under pressure into the moulds. Therefore, the resolution of the injected parts is dependent on the precision of the mould manufacturing [30].

3.3. Cold Pressed Body Machining- CPBM

Uniaxial cold-pressing is the traditional way for shaping and consolidation of ceramic materials. Ceramic powders are formed into shapes in dies using hydraulic presses. This is done to impart the sufficient strength to the part to enable handling for further processing. The pressed powder is known as "green compact". However, due to the presence of friction between the ceramic particles in the powder and the friction between the punches and the die walls, there can be considerable variation in density within the part [31]. The powder can be compacted without additives or with the use of a small amount of polymer as a binder to ensure the required shape stability. Different materials and particle sizes can also be used to reduce friction. The ceramic material after sintering is very brittle, therefore the substrates are manufactured as green compacts with a small amount of binder and subsequently machined into the final emitter geometries. The advantage of this method is the possibility of using a variety of powders with different grain sizes which have a significant influence on the final porosity of the parts. The porosity is also influenced by the amount of binder addition (the higher addition, the higher porosity level and larger pores) or by the pressure used for consolidation. Generally, pressures up to 200 – 300 MPa are efficient. A picture of the first single emitters shaped by machining of a cold-pressed body are shown in Figure 4.

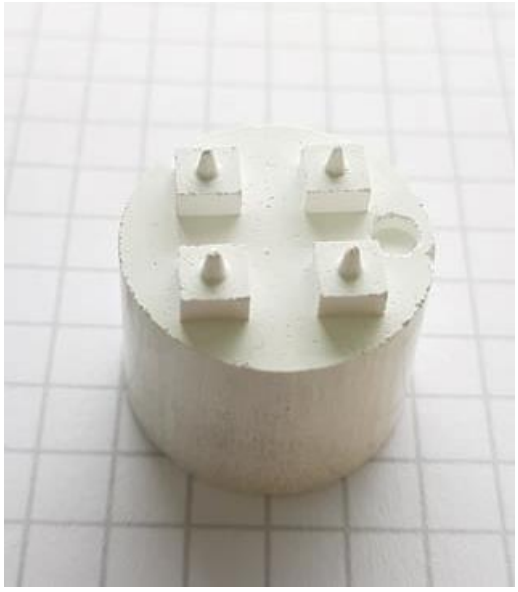

Figure 4: Single emitters prepared by machining of a cold pressed green body.

4. High Voltage Power Processing Unit (HV-PPU)

The thruster's overall technology readiness level is dependent on the HV-PPU which energizes the PET-50 by generating the regulated and conditioned supply voltages required by the electrodes. This consortium's high voltage PPU generates up to ±3.5 kV from a 12 V CubeSat bus voltage. A simplified schematic of the PPU is depicted in Figure 5.

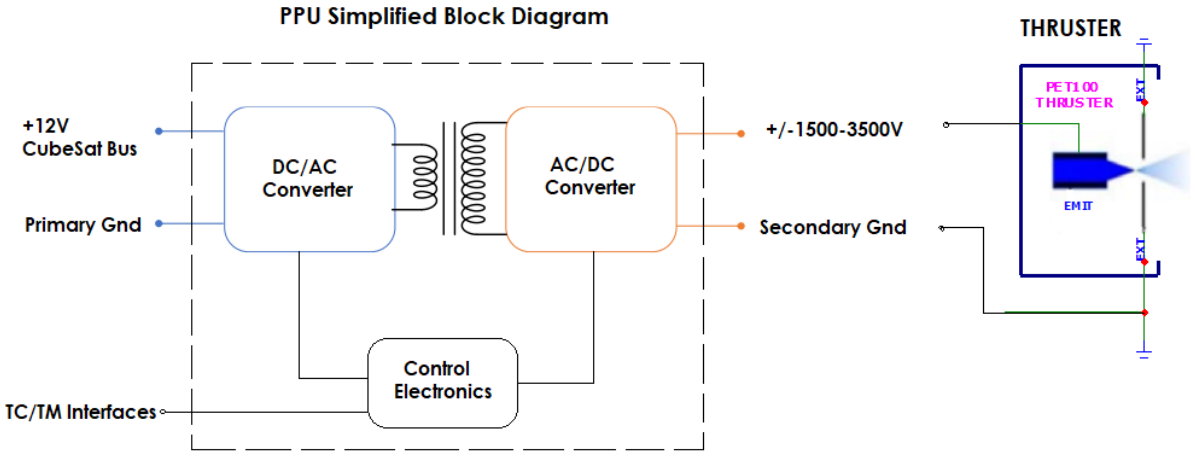

Figure 5: Schematic of the HV-PPU under development.

The baselined PPU has two main sections: a power section and a control electronics section. The power section is made up of a DC/AC converter, a transformer, and an AC/DC rectifier. The DC/AC converter is used to convert the 12V DC from the CubeSat bus to an AC power pulse which is then applied across a HV transformer with adequate step-up ratio to convert it to an intermediate AC voltage. The AC/DC rectifier stage uses multiple Cockcroft-Walton (CCW) High-Voltage (HV) stages to generate the high voltages up to ±3.5 kV as required by the PET-50 electrodes. The control electronics generate the Pulse Width Modulation (PWM) signals required to drive the DC/AC converter and compute the Proportional Integral Derivative (PID) loops. The control electronics will also include the necessary functions for telecommand, telemetry (health monitoring) and protection of the overall thruster system.

5. Experimental Apparatus and Pre-test Preparations

For the PET prototype only the current-voltage characteristics were recorded alongside long exposure photographs, based on work by ref [32]. These were taken as supplementary data to ensure the thruster was not sparking and to complement the current-voltage data in characterising the emitter operation. Prior to manufacturing a large array of emitters, single emitters were tested to ensure good current emission.

5.1. Vacuum Facility

The PET-50 test campaigns are being carried out in the David Fearn Electric Propulsion Laboratory located at the University of Southampton. The laboratory contains a high-quality vacuum system manufactured by Cutting Edge Coatings GmbH, as shown in Figure 6.

Figure 6: The vacuum system in the David Fearn Electric Propulsion Laboratory at the UoS.

The vacuum system consists of a small 70 cm diameter/70 cm length chamber, fitted with a roughing pump and a turbo-pump with a pumping rate of 2100 L/s of N_2. These can bring the pressure down to 5.6 x 10^{-5} mbar, which is sufficient for the initial testing of nanosatellite-class electrospray thrusters as they usually have relatively low mass flow rates.

5.2. PET Electrospray Single Emitter Setup

The first set of experiments were performed using additively manufactured single emitter prototypes, to test the manufacturing method and electrospray performance. Conical emitters of smaller (see Figure 7) and larger (not shown here) tip radii were used for the initial investigation. The single-tip emitter electrospray thruster used is shown in Figure 8. The core parts of the thruster are the porous emitter which is in contact with a porous reservoir. These are both then encased. The thruster casing was 3D printed using Formlabs Rigid Resin 4000, procured from Protolabs Hubs. A bolt through the back of the casing was connected to the rear surface of the reservoir, working the electrical connection to the power supply. The thruster has a size of around 3 x 3 x 4 cm. The extractor plate is made of AISI 316 stainless steel, with an aperture of 1.0 mm diameter. The distance between emitter tip and extractor upstream surface was approximately 200 μm.

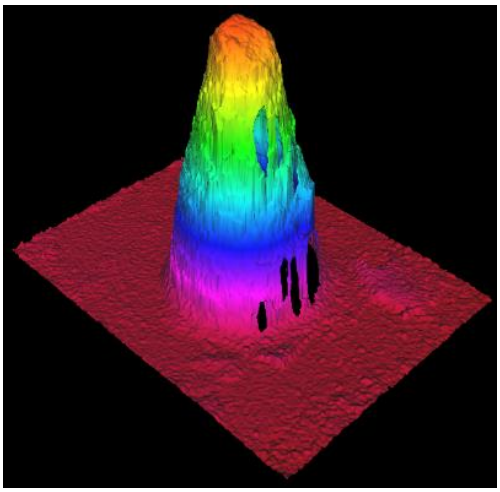

Figure 7: Smaller radius additively manufactured single conical emitter.

Figure 8: Thruster housing for a single emitter tip, comprised of an extractor plate with a single aperture and a porous reservoir.

5.3. PET Current Measurement System

Typically several kilovolts are required to operate the PET to achieve spray onset and emit charged particles. For most of the current electrospray thruster testing, desktop power supplies were used whilst we concurrently developed the HV-PPU. In this research, the high voltage (i.e. the emitter potential) was supplied by two HCP 35-3500 models that provide $\pm$ 3500 V and up to 10 mA of current, both sourced from FuG Elektronik GmbH. The thruster is tested in a bipolar mode where the emitter polarity was switched periodically to mitigate electrochemical effects [33, 34, 35]. The polarity switching is achieved using a high voltage switching unit made at the University of Southampton, which has several mechanical reed switches to alter the output voltage between two opposite-polarity voltage inputs, following the frequency of a square wave from a function generator.

In order to evaluate the performance of PET, the collector current and extractor current are collected. The collector current corresponds to the total current of charged particles emitted out of the thruster into space and is measured using a downstream plume collector. The plume collector is manufactured from an AISI 316 20cm x 20cm plate with a Secondary Electron Emission suppression (SEE) grid procured from Precision e-forming placed 5 mm above the plate. The SEE grid is charged to -100V throughout testing, so that SEE is completely negated. To record the current incident on the collector plate, a Femto DHCPA-100 'Fast-amp' is used to provide amplification and conversion from a current to a voltage signal. The fast-amp is connected to a Picoscope 2202 which is used to convert the voltage signal and record it on a computer. The extractor current, which is the current produced by impinging ions on the extractor, is recorded using a 0.9092 MΩ resistor which was connected outside the vacuum chamber between the extractor and the ground. The voltage drop of the resistor during the electrospray emission was measured using an ISO-TECH IDM 507 multimeter. Finally, the extractor current is calculated using Ohm's law. The testing set up is illustrated in Figure 9. For long exposure photography a DSLR (Canon EOS 250D) was used. This was set to ISO 12800 with an exposure time of 30s. This configuration was found empirically to work well with the extremely low emission of light in University of Southampton PETs.

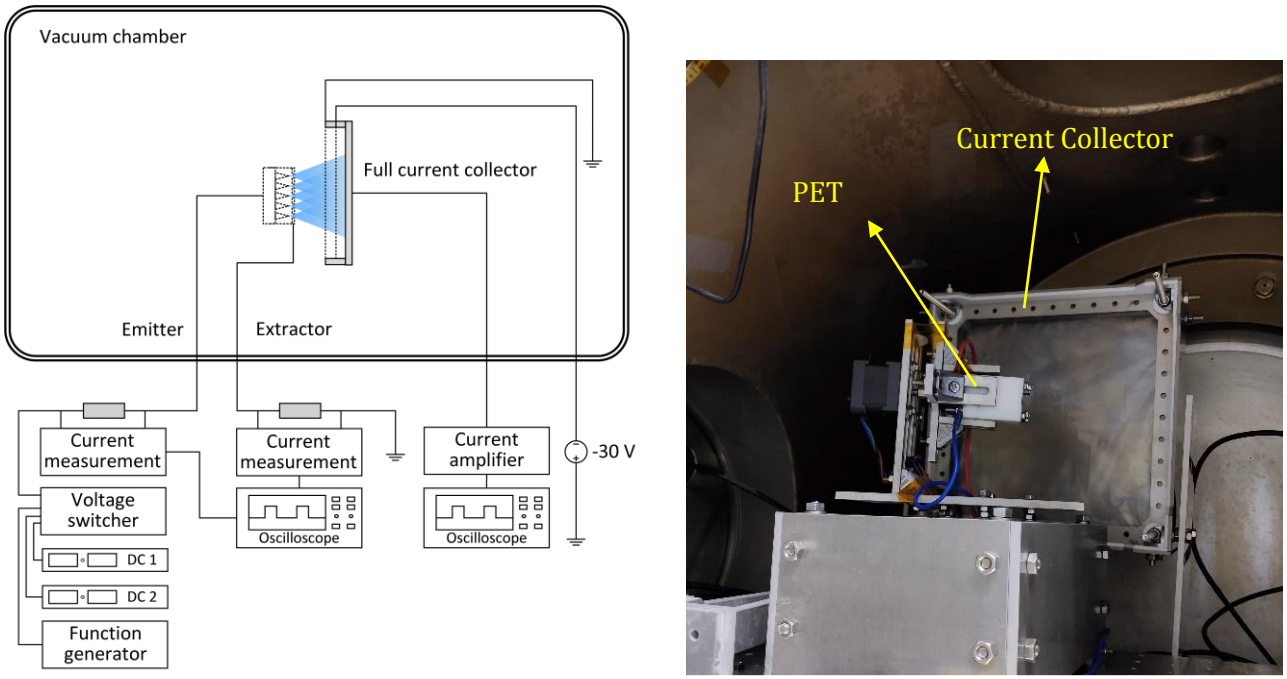

Figure 9: Illustration of the current measurement system setup [22].

5.4. Pre-test Thruster Preparations

5.4a Ionic Liquid Purification

The EMI-BF_4 ionic liquid propellant tested in this research was sourced from Sigma-Aldrich Corporation. The product came with a concentration of 99.0% and the impurities were mainly water with a concentration of <200 mg/kg. In order to eliminate the water impurities, the ionic liquid baths were put through vacuum depressurization procedures, allowing the water to evaporate from the solutions before they were used to fill the emitters and reservoirs. The approach taken was pulling approximately 30 ml into a beaker, which was then depressurized to the level of 10^{-2} mbar. In the low-pressure environment, the ionic liquid baths were found to be experiencing violent bubbling due to rapid vaporization of water. The vacuum was maintained at these low pressures for 30 minutes to 2 hours until no more bubbling occurred in the liquid bath and the descending pressure readings of the vacuum chamber reached a stable state without random pulsed increases, indicating that the majority of the water impurities in the ionic liquid had evaporated.

5.4b Preparation of Porous Material Substrates

The porous material substrates, including the emitter and the reservoir, were cleaned before being adequately filled with ionic liquid propellant. Following additive manufacturing, the porous substrates contain various impurities on and inside the material. These impurities can include sintered material powders for example. In order to eliminate impurities, the substrates were cleaned using two procedures. Firstly an ultrasonic bath was used to remove material on the surface of the emitter. The temperature of the bath was set to 30 ^{0}C. Depending on the size of the porous substrate, each soaking process took 30 minutes to 2 hours. Note, ultrasonic cleaning in a deionized water bath cannot effectively remove organic liquid residues on the porous material surface. To achieve this the substrates were washed thoroughly using acetone or isopropyl alcohol (IPA). Although acetone and propane are highly volatile, there could still be water contained in the porous material which would compromise the concentration of the ionic liquid propellant once it is filled. In order to avoid this problem, the porous substrates were put in the vacuum chamber down to pressures of approximately 1x 10^{-4} mbar. The low pressure was maintained for 2 to 4 hours until the chamber pressure remained stable while not experiencing sudden increases for several minutes, allowing the majority of the water trapped in the porous materials to evaporate.

After these two cleaning procedures, the porous material substrates were filled with ionic liquid in preparation for testing. For the filling, the porous substrates were immersed in the ionic liquid solution in a beaker which was then put in the vacuum for another 30-minute to 1-hour long depressurization, allowing the air voids to vent out from the substrates. Subsequently, the beaker was taken out from the vacuum, and the substrates were removed from the ionic liquid bath.

Excessive ionic liquids on the substrate surfaces were gently cleaned using high-absorbance cleaning papers. After this step, the porous emitters and reservoirs were assembled in the thruster housing.

6. Preliminary Results

The current-voltage curves for both the emitters are shown in Figure 10 and Figure 11 respectively. The emitter with smaller tip radius had an onset voltage of around ± 1850 V (Figure 10), while the larger tip had a higher onset voltage of approximately ± 2200 V (Figure 11). Although needing a higher voltage to initiate current emission, the current emitted by the larger tip increased more rapidly with voltage than the smaller one. The maximum emission current from the larger radius emitter went up to 30 µA and -35 µA at ± 3500 V (Figure 11) while the smaller tip emitter reached 28 µA and -25 µA at ± 3500 V (Figure 10).

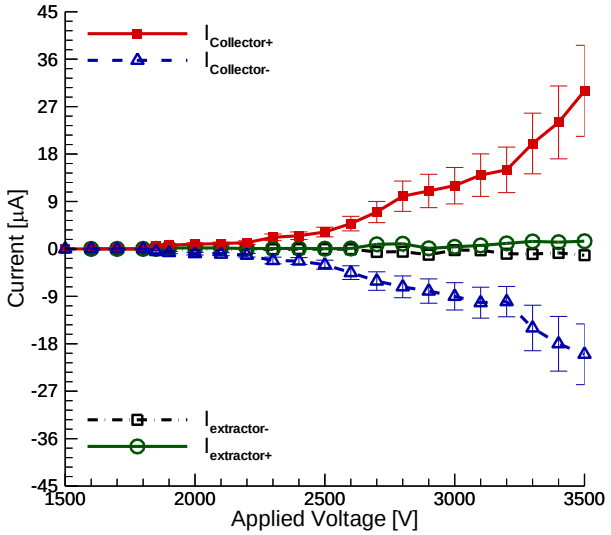

Figure 10: Measured collector and extractor current versus emitter voltage. Smaller tip radius.

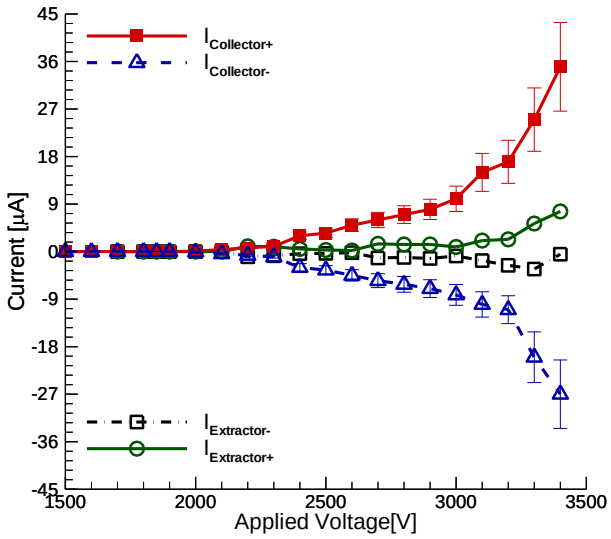

Figure 11: Measured collector and extractor current versus emitter voltage. Larger tip radius.

Interestingly, when the thruster voltage was less than ± 3100 V, the extractor current was found to be smaller than 10% and would not affect the stable operation of the thruster. However, when the thruster voltage was increased to ± 3500 V, the extractor current significantly increased, marked by sharp glow in the thruster as shown in Figure 12. This may be an effect relating to secondary species emission [32, 37].

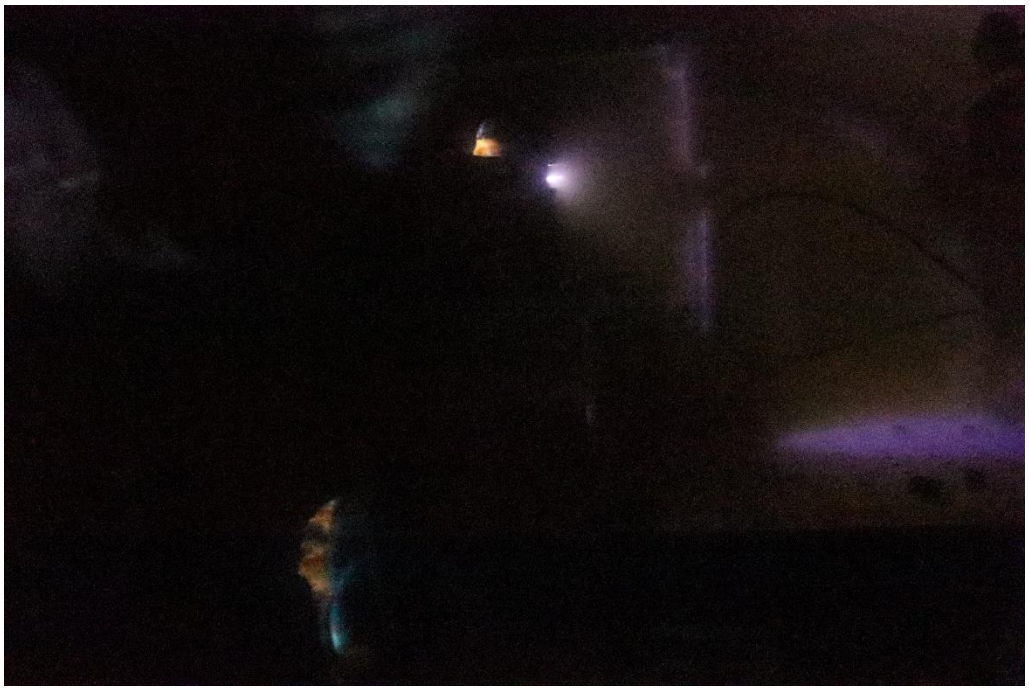

Figure 12: Glowing phenomenon observed in PET electrospray single emitter, at ± 3500 V. The plume of the thruster is clearly visible in front of the extractor of the thruster. The plume can be traced to the vacuum chamber bottom, where it forms a glowing circular patch.

The current per emitter strongly relates to the thrust per unit area, which is a crucial factor determining the effectiveness of an electrospray thruster. Compared with most electrospray thruster porous emitters being developed [19, 24, 37], both PET thrusters showed relatively high emission current per emitter, demonstrating the PET electrospray thrusters show promise they will achieve high overall emission current and thrust. Assuming a 50 % - 50 % monomer-dimer mix, the estimated thrust per emitter F_{pe} is ~3.48 μN for the larger tip and ~2.40 μN for the smaller tip with nearly similar I_{sp} ~ 4600 s at 3.50 kV. For the PET-50 operating with these novel emitter arrays, the number of emitter tips required for each PET unit is N_{em} ~ 72-100 producing a thrust of $F_{pet.}$ ~250 μN with an input power of P_{pet} ~ 9 W. Four thruster units operating together can achieve mission total thrust of F_T ~ 1 mN consuming only ~36 W, well below the target value.

7. Summary and Future Work

This research work has described an ongoing effort to develop a high-performance electrospray thruster for nanosatellite applications. The PET thruster, previously developed at UoS, is being improved in collaboration with AVS UK and RHP Technology Austria. The goal being to achieve higher thrust to power ratio with a design suitable for high volume production, thus satisfying nanosatellite market demand. The UoS is leading the testing as well as contributing to the design of the thruster, while RHP Technology is manufacturing the porous emitter arrays and the reservoirs. AVS UK is responsible for the design of a flight ready thruster, is developing the associated Power Processing Unit (PPU), and is leading the end commercial exploitation of the technology. Importantly, the emitter manufacturing technique has changed from CNC machining to the use of sintering in order to avoid issues with non-uniform emission.

The preliminary results have demonstrated the stable operation of additively manufactured porous emitters, through repeatable tests with reasonably high emission currents. Further emitters have been manufactured and will be tested in June 2022. Electrical diagnostics, including retarding potential analysis and time of flight measurements, will be conducted on the new emitters. The authors will investigate the effect of varying onset voltage and emitter-extractor geometrical parameters on thruster's performance. A detailed overall design for a breadboard PET thruster has been completed, and testing of this breadboard will occur in late summer 2022.

References

[1] M. N. Sweeting, "Modern small satellites—Changing the economics of space," *Proc. IEEE,* vol. 106, no. 3, pp. 343-361, 2018.

[2] M. Knapp, S. Seager, B. O. Demory, A. Krishnamurthy, M. W. Smith, C. M. Pong, V. P. Bailey, A. Donner, P. D. Pasquale, B. Campuzano, C. Smith, J. Luu, A. Babuscia, R. L. Bocchino Jr, J. L. C. Colley, T. Gedenk, T. Kulkarni, K. Hughes, M. White, J. Krajewski and L. Fesq, "Demonstrating High-Precision Photometry with a CubeSat: ASTERIA Observations of 55 Cancrie," *Astronomical Journal,* vol. 23, 2020.

[3] E. Gill, P. Sundaramoorthy, J. Bouwmeester, B. Zandbergen and R. Reinhard, "Formation Flying with in a Constellation of Nano-Satellites: The QB50 Mission," *Acta Astronautica,* vol. 82, pp. 110-117, 2013.

[4] Klesh at. al., "Inspire: Interplanetary NanoSpacecraft Pathfinder In Relevant Environment," in *Proceedings of the AIAA SPACE 2013 Conference and Exposition*, San Diego, CA, USA, 10–12 September, 2013.

[5] A. R. Tummala and A. Dutta, "An Overview of Cube-Satellite Propulsion Technologies and Trends," *Aerospace,* vol. 4, no. 58, 2017.

[6] L. Brieda, D. B. Zolotukhin and M. Keidar, "PIC-DEM Modelling of Vacuum Arc Thruster Electrodes," in *AIAA Propulsion and Energy Forum*, 2021.

[7] S. Chowdhury and I. Kronhaus, "Characterization of Vacuum Arc Thruster Performance in Weak Magnetic Nozzle.," *Aerospace,* vol. 7, no. 82, 2020.

[8] I. Kronhaus, M. Laterza and A. R. Linossier, "Experimental Characterization of the Inline-Screw-Feeding Vacuum-Arc-Thruster Operation," *IEEE Transactions on Plasma Science,* vol. 46, no. 2, pp. 283-288, 2018.

[9] D. Lev, R. M. Myers, K. M. Lemmers, J. Kolbeck, H. Koizumi and K. Polzin, "The technological and commercial expansion of electric propulsion," *Acta Astronautica,* vol. 159, 2019.

[10] M. J. Patterson, J. E. Foster, J. A. Young and M. W. Crofton, "Annular Engine Development Status," in *Joint Propulsion Conference*, San Jose, CA: American Institute of Aeronautics and Astronautics, 2013.

[11] M. J. Patterson, R. Thomas, M. W. Crofton, J. A. Young and J. E. Foster, "High Thrust to Power Annular Engine Technology," in *Joint Propulsion Conference*, Orlando FL: American Institute of Aeronautics and Astronautics, 2015.

[12] G. Quinsac, B. Segrea, C. Koppel and B. Mosser, "Attitude control: A key factor during the design of low thrust propulsion for CubeSats," *Acta Astronautica,* vol. 176, 2020.

[13] L. Grimaud and S. Mazouffre, "Performance comparison between standard and magnetically shielded 200 W Hall thrusters with BN-SiO2 and graphite channel walls," *Vacuum,* vol. 155, pp. 514-523, 2018.

[14] D. Krejci, F. M. Hicks, C. Fucetola, P. Lozano, A. H. Schouten and F. Martel, "Design and Characterization of a Scalable Ion Electrospray Propulsion System," in *Presented at Joint Conference of 30th International Symposium on Space Technology and Science, 34th International Electric Propulsion Conference and 6th Nano-satellite Symposium*, Hyogo-Kobe, Japan, 2015.

[15] K. Lemmer, "Propulsion for CubeSats," *Acta Astronaut.,* vol. 134, pp. 231-243, 2017.

[16] R. S. Legge, E. B. Clements and A. Shabshelowitz, "Enabling microsatellite maneuverability: A survey of microsatellite propulsion technologies," in *In Proceedings of the 2017 IEEE MTT-S International Microwave Symposium (IMS)*, Honololu, HI, USA, 2017.

[17] D. Spence, E. Ehrbar, N. Rosenbald, N. Demmons, T. Roy, S. Hoffman, W. D. Williams, M. Tsay, J. Zwahlen and K. Hohman, "Electrospray Propulsion Systems for Small Satellites," in *AIAA SPACE 2013 Conference and Exposition*, San Diego, CA, USA, 2013.

[18] "Enpulsion, 'Introduction to the IFM Nano Thruster" [Online]. Available: http://www.enpulsion.com/uploads/ENP-IFMNanoT," 2017.

[19] M. R. Natisin and H. L. Zamora, "Performance of a Fully Conventionally Machined Liquid-Ion Electrospray Thruster Operated in PIR," in *IEPC-2019-522, Presented at the 36th International Electric Propulsion Conference*, University of Vienna, Austria, September 15-20, 2019.

[20] C.Ma and C.Ryan, "Plume Particle Energy Analysis of an Ionic Liquid Electrospray Ion Source with High Emission Density," *Journal of Applied Physics*, vol. 129, 2021.

[21] C. Ma and C. Ryan, "Plume Characterization of a Porous Electrospray Thruster," in *IEPC-2019-A223, Proceedings of the 36th International Electric Propulsion Conference*, 2019.

[22] C. Ma, "Design and Characterisation of Electrospray Thrusters with High Emission Density," *PhD Thesis, University of Southampton, Department of Aeronautical and Astronautical Engineering,* pp. 1-275, 2019.

[23] C. Ma, T. Bull and C. N Ryan, "Plume Composition Measurements of a High-Emission-Density Electrospray Thruster," *Journal of Propulsion and Power,* 2021.

[24] D. G. Courtney, N. Alvarez and N. R. Demmons, "Electrospray Thrusters for Small Spacecraft Control: Pulsed and Steady State Operation," in *Joint Propulsion Conference, ser. AIAA Propulsion and Energy Forum.*, American Institute of Aeronautics and Astronautics, 2018.

[25] M. Tsay and D. G. Courtney, "All- Electric CubeSat Propulsion Technologies for Versatile Mission Applications," in *32nd International Symposium of Space Technology and Science*, Fukui, Japan, 2019.

[26] A. A. Rashid, S. A. Khan, S. G. Al-Ghamdi and M. Koc, "Additive Manufacturing: Technology, Applications and Markets," *Automation in Construction,* pp. 1-18, 2020.

[27] G. Goh, G. Agarwala, G. Goh, V. Dikshit and W. Yeong, "Additive Manufacturing in Unmanned Aerial Vehicles (UAVs): Challenges and Potential," *Aerospace Science and Technology,* pp. 1-36, 2016.

[28] F. Melchels, J. Feijen and D. Grijpma, "A Review on Stereolithography and its Applications in Biomedical Engineering," *Biomaterials,* vol. 31, pp. 6121-6130, 2010.

[29] T. Moritz and S. Maleksaeedi, "4-Additive Manufacturing of Ceramic Components," *Additive Manufacturing Materials, Processes, Quantifications and Applications*, pp. 105-161, 2018.

[30] J. G. Gutierrez, G. B. Stringari and I. Emri, "Powder Injection Molding of Metal and Ceramic Parts," *Some Critical Issues for Injection Molding,* pp. 665-688, 2012.

[31] G. Hammes, C. Binder, A. Galiotto, A. N. Klein and H. A. Al-Qureshi, "Relationship Between Cold Isostatic Pressing and Uniaxial Compression of Powder Metallurgy".

[32] N. Uchizono and R. Wirz, "Facility Effects for Electrospray Thrusters," in *AIAA Scitech Forum*, San Diego, 2022.

[33] K. Msuyama and P. C. Lozano, "Electrical Double Layers in Electrospray Propulsion," in *34th International Electric Propulsion Conference*, Kobe, Japan, 2015.

[34] P. C. Lozano and M. M. Sanchez, "Ionic Liquid Ion Sources: Suppression of Electrochemical Reactions Using Voltage Alternation," *Journal of Colloid and Interface Science*, vol. 280, pp. 149-154, 2004.

[35] K. Masuyama, "Electrochemistry of Room Temperature Ionic Liquids with Application to Electrospray Propulsion," *Ph.D. Dissertation, MIT, USA*, 2016.

[36] N. Uchizono, A. Collins, C. M. Reading, S. Arestie, J. Ziemer and R. Wirz, "The Role of Secondary Species Emission in Vacuum Facility Effects for Electrospray Thrusters," *Journal of Applied Physics*, vol. 130, 2021.

[37] D. Krejci, F. Mier-Hicks, R. Thomas, T. Haag and P. Lozano, "Emission Characteristics of Passively Fed Electrospray Microthrusters with Propellant Reservoirs," *Journal of Spacecraft and Rockets*, vol. 54, no. 2, pp. 447-458, 2017.